UTILITAS MATHEMATICA 122 (2025) 3–27

Utilitas Mathematica
www.combinatorialpress.com/um

Combinatorial Press

Double bond indices and their application: QSAR of polycyclic aromatic hydrocarbons

Harsha Vardhan K S[1], Anuradha D S[2], Jaganathan B[2,✉]

[1] *Department of Computer Science, Vellore Institute of Technology, Chennai, India*

[2] *Department of Mathematics, Vellore Institute of Technology, Chennai, India*

ABSTRACT

Topological Indices (TIs) are quantitative measures derived from molecular geometry and are utilized to predict physicochemical properties. Although more than 3000 TIs have been documented in the published literature, only a limited number of TIs have been effectively employed owing to certain limitations. A significant drawback is the higher degeneracy resulting from the lower discriminative power. TIs utilize simple graphs in which atoms and bonds are conceptualized as the vertices and edges of mathematical graphs. As multiple edges are not supported in these graphs, double and triple bonds are considered single. Consequently, the molecular structure undergoes alterations during the conversion process, which ultimately affects the discriminative power. In this investigation, indices for double-bond incorporation were formulated to preserve structural integrity. This study addresses, demonstrates, and verifies a set of double-bonded indices. The indices demonstrated promising results, exhibiting enhanced discriminative power when validated for polycyclic aromatic hydrocarbons using regression analysis. These indices and their potential applications will significantly contribute to QSAR/QSPR studies.

Keywords: double bonds, degree-based indices, new indices, polycyclic aromatic hydrocarbons, regression analysis, QSAR/QSPR

2020 Mathematics Subject Classification: 05C69.

1. Introduction

Topological indices is the final result of a logic and mathematical procedure which transforms chemical information encoded within a symbolic representation of a molecule into a useful number or the result

✉ Corresponding author.
E-mail address: jaganathan.b@vit.ac.in (Jaganathan B.)

Received 09 January 2025; accepted 04 March 2025; published 22 March 2025.

DOI: 10.61091/um122-01

of some standardized experiment-Todeschini & Consonni [54].

Topological indices are interdisciplinary research that apply graph theory concepts (mathematics) to the molecular structures of chemical compounds. They have a wide range of applications in pharmaceutical sciences, material studies, nanostructures, and many others through quantitative structure-property/activity relationship (QSAR) [10]. Topological analysis of molecular structures yields numerical descriptors or polynomials that reflect atomic interconnectivity. These mathematical representations, derived from the chemical topographic structure, can be expressed as simple graphs. The underlying principle relies on the binary relationships between atoms within the molecular framework [35]. Simple graphs were constructed by depicting the atoms as vertices, and the bonds in the constitutional formulas were represented as edges [2]. In these simple chemical graphs, the type of bond is neglected, that is, all double and triple bonds are considered single bonds [36]. The resonance phenomenon constitutes the primary rationale for disregarding double and triple bonds [35]. Resonance, a fundamental chemical concept, describes the representation of a single molecular entity as a composite of multiple electronic structures, wherein the atomic arrangement remains constant while the electron distribution varies [55]. Therefore, to mitigate the uncertainty associated with bond positioning during the calculation of TIs, researchers have excluded double and triple bonds from consideration. For instance, the resonance phenomenon in Naphthalene, a compound comprising two benzene rings, exhibits two contributing structures, as in Figure 1.

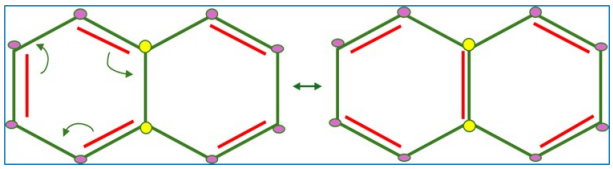

Fig. 1. Resonance – Naphthalene

Thus, the position of the bonds resonates within the chemical compound, as in Figure 2.

Topological indices (TIs) are primarily classified into two categories: those based on distance and those based on degree. The pioneering TI, known as the Wiener index W(G), falls under the distance-based category and was first introduced by Wiener in 1947. This index was formulated using a set of numerical values derived from the distances between vertices (atoms), which were calculated by determining the minimum number of edges (bonds) separating any two atoms [17]. It can be easily understood that the minimum distance between any two atoms remains the same irrespective of the nature(single/double) of the bond. This negligence does not affect the correlation ability of distance-based TIs.

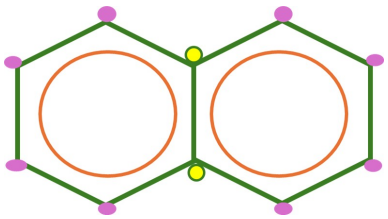

Fig. 2. Representation of resonance-Naphthalene

The quantity of edges incident on any atom is known as the vertex degree, which corresponds to the valence of the atom in any molecular structure [3]. A wide range of degree-based indices, such as Sombar and Zagreb, have been developed to predict the physiochemical features of a group of

chemical compounds [22, 50, 8]. As per survey, approximately 3000 indices have been formulated https://onlinelibrary.wiley.com/doi/toc/10.1155/1469.si.474120.

However, a few well-established TIs have been widely used because of a few drawbacks. One of these is the degeneracy created by the less discriminative power of TIs. Degeneracy occurs when the same TI value is obtained for two different molecular structures. For instance, the numerals obtained for cyclohexane and benzene were the same when calculated for any TI. This is because during the conversion of a chemical compound to a simple graph, the structure of the molecule is not retained because the double bonds are considered single bonds. The simple graph of both molecules possesses the same structure, as shown in Table 1.

Table 1. Simple Graph of Cyclohexane and Benzene

Chemical Compound	Molecular Structure	Simple Graph
Cyclohexane(C_6H_{12})		
Benzene(C_6H_6)		

To address this issue, a literature survey was performed on TIs, their new formulations, and the molecular structures used to validate these TIs. The survey ensured the necessity of formulating indices that incorporate double bonds. Further investigation of various other sets of chemical compounds is necessary to enable the practical use of TIs in the field of QSAR/QSPR. In this study, new indices incorporating double bonds were evaluated for polycyclic aromatic compounds(PAHs) using an edge partition technique. These proposed indices use the concept of duplicate graphs, which has never been explored previously in chemical graphs. Therefore, the process of edge partitioning using these simple and duplicate graphs is illustrated using the naphthalene structure. The results are used to envisage the properties specifically, Boiling Point(BP), Flash Point(FP), Enthalpy of Vaporization (EV), Index of Refraction(IR), Polarizability(Pol), Octanol water partition coefficient (Log P), Surface Tension(ST), Molar Mass(MM), Molar Volume(MV), Retention Index(RI), Molecular Weight(MW), X log P3-AA, Heavy Atom Count(HAC), and Complexity. Predictions were validated using linear and quadratic regression analyses. The analysis is portrayed visually, and the prospects of the study are discussed in the final section. The results of this study would make a substantial difference in QSAR/QSPR studies, thereby increasing the practical use of TIs in virtual screening of lead compounds.

1.1. Research necessity

The extant literature reveals a paucity of topological indices (TIs) capable of accommodating multiple bonds, with only a select few—namely Sze, X, J, w, and IDW functioning as edge-weighted and vertex-weighted indices [14]. These TIs encapsulate fundamental atomic properties, including atomic number, electronegativity, van der Waals area and volume, and covalent radius [30, 25, 26, 6]. Formulated using vertex-adjacency and atom-connectivity matrices of multigraphs, these indices necessitate an evaluation of their predictive efficacy to broaden their applicability [28]. Notably, a comprehensive analysis of multigraph indices for elucidating the general physicochemical characteristics of chemical compounds remains unexplored. The past decade and a half have witnessed a conspicuous absence of extensive research on chemical structures utilizing multigraph-based TIs [48, 27, 44, 39, 60, 58, 56, 41, 4, 47, 61, 16, 9, 29, 21, 12, 40, 31, 23, 32, 42, 43, 15, 57]. Current

research methodologies fail to account for resonant structures, prompting the integration of novel formulations into established degree-based indices to encompass double bonds. These refined indices may prove instrumental in mitigating degeneracy in future studies involving diverse sets of chemical compounds.

1.2. Literature survey

In literature, new formulations are given for existing TIs [37, 1] aimed at enhancing their discriminative power [45]. These proposed TIs undergo validation through regression analysis and various chemical compound sets, with a focus on Polycyclic Aromatic Hydrocarbons (PAHs). Notable examples include the theta, Pi and Sadhana indices, eccentricity-based topological indices [50], Neighbourhood eccentricity-based indices [59], two novel temperature-based TIs [19], elliptic Sombar index and connection number-based Zagreb indices are validated using PAHs for QSAR/QSPR models [34]. A multitude of PAHs exists such as Dodeca-benzo -circumcorenene [52], Hexa-peri-hexabenzocoronene, Hexa-cata -hexabenzocoronene [50] with numerous others [51, 59, 34, 38, 5, 20] predicted using TIs. In PAH assessment, the generalized Randić and sum-connectivity indices demonstrate significantly higher efficiency compared to other established degree-based indices [34]. However, a trade-off exists as efficient TIs often exhibit reduced discriminative power. This allows for a meaningful comparison between newly developed and existing indices for PAHs. Specific PAH compounds are chosen for validation, as detailed in subsequent sections.

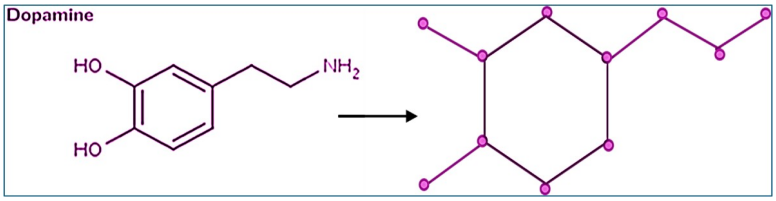

Fig. 3. Structure of Dopamine and its corresponding Simple Graph

1.3. Duplicate graph

E. Sampath Kumar first proposed the concept of a duplicate graph of the parent graph in 1974. It is possible to create a duplicate graph from every finite, undirected graph [46]. Such duplicate graphs are widely employed in graph labelling techniques [53, 13, 24]. Let $\mathfrak{G}(V, \mathfrak{V})$ be a simple graph with l number of vertices and a total of m edges. A duplicate graph $\mathfrak{G}_d(A, B)$ of $\mathfrak{G}$ contains two sets of vertices and two sets of edges satisfying (i)$A = V \cup V'$ and $\phi = V \cap V'$, where $\xi : V \to V'$ is a bijective relation (ii) $B = E_i/e_i\&e_(i^{'}\prime) \in B$, where $i = 1, 2 \ldots m$ [24]. An illustration of a duplicate graph of butane is portrayed in Figures 4 to 6.

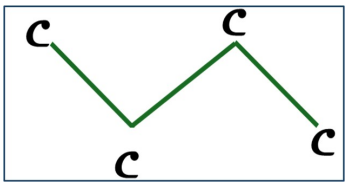

Fig. 4. Molecular Structure of Butane

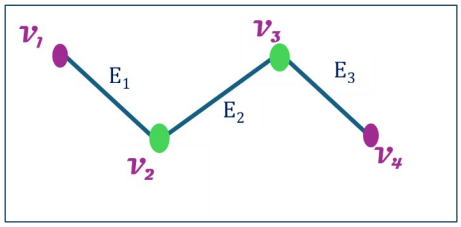

Fig. 5. Simple Graph of Butane (4 vertices, 3 edges)

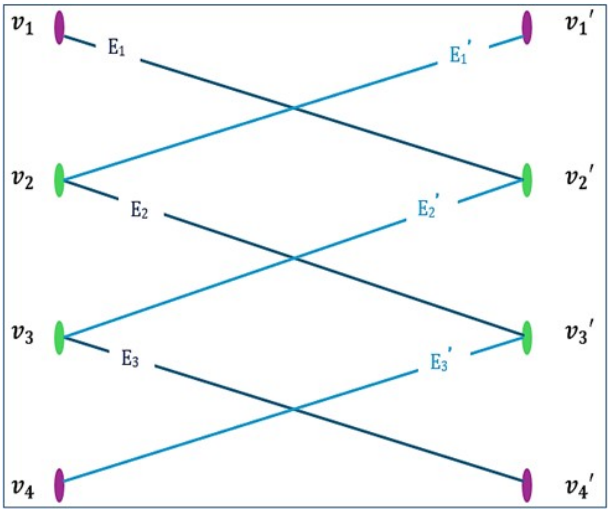

Fig. 6. Duplicate Graph of Butane (8 vertices, 6 edges)

2. Main results

2.1. New extended double bond indices

Any molecular structure was converted into a simple graph to compute TIs. Duplicate graphs are employed along with simple graphs to formulate the double bond TIs in the following steps: (a) The duplicate graph of the considered molecular structure is drawn from the simple graph (b) The weights $1, 0, w_i$ are assigned to the edges of the duplicate graph according to their correspondence with the molecular structure. (c) The edge partitioning technique is used to duplicate graphs. The process of calculating the double-bond indices is shown in Figure 7.

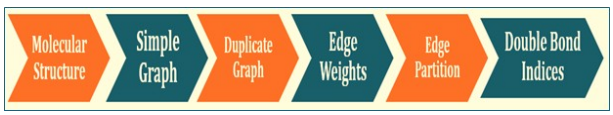

Fig. 7. Evaluation Process of Double Bond Indices

These formulated indices incorporate double bonds when different weights are added to different categories of edges in the duplicated graph. As a result, both the actual structure of the chemical compound and the mathematical characteristics of the graph were maintained during the entire process. The formulation of the double-bond degree-based TIs and their symbolization are listed in Table 2.

In the formulation W_i, takes three different values $1, 0, \theta_i$ according to their correspondence with the molecular structure. where $\theta_i = \tau_i/N, \tau_i =$ Number of parallel edges in each edge partition and N is the total edge cardinality. Because these indices have not been explored in detail, an illustration

of the molecular structure of naphthalene is presented. The molecular structure of naphthalene and its corresponding simple graphs are shown in Figure 8.

Table 2. Formulas for Different Topological Indices

S.No.	Symbol	TIs	Formulation
1	IS^D	Inverse Sum Indeg Index - Double	$\sum_{e\in E(Y)}\left(\frac{d_\sigma d_\tau}{d_\sigma+d_\tau}\right)+w_i\sum_{e'\in E(Y')}\left(\frac{d_\sigma d_\tau}{d_\sigma+d_\tau}\right)$
2	M^2R^D	Min-Max Roder Index - Double	$\sum_{e\in E(Y)}\sqrt{\frac{\min\{d_\sigma,d_\tau\}}{\max\{d_\sigma,d_\tau\}}}+w_i\sum_{e'\in E(Y')}\sqrt{\frac{\min\{d_\sigma,d_\tau\}}{\max\{d_\sigma,d_\tau\}}}$
3	M^2RD^D	Max-Min Roder Index - Double	$\sum_{e\in E(Y)}\sqrt{\frac{\max\{d_\sigma,d_\tau\}}{\min\{d_\sigma,d_\tau\}}}+w_i\sum_{e'\in E(Y')}\sqrt{\frac{\max\{d_\sigma,d_\tau\}}{\min\{d_\sigma,d_\tau\}}}$
4	SDD^D	Symmetric Division Degree Index - Double	$\sum_{e\in E(Y)}\left(\frac{\min\{d_\sigma,d_\tau\}}{\max\{d_\sigma,d_\tau\}}+\frac{\max\{d_\sigma,d_\tau\}}{\min\{d_\sigma,d_\tau\}}\right)+$ $w_i\sum_{e'\in E(Y')}\left(\frac{\min\{d_\sigma,d_\tau\}}{\max\{d_\sigma,d_\tau\}}+\frac{\max\{d_\sigma,d_\tau\}}{\min\{d_\sigma,d_\tau\}}\right)$
5	SC^D	Sum Connectivity Index - Double	$\sum_{e\in E(Y)}\frac{1}{\sqrt{d_\sigma+d_\tau}}+w_i\sum_{e'\in E(Y')}\frac{1}{\sqrt{d_\sigma+d_\tau}}$
6	ABC^D	Atom Bond Connectivity Index - Double	$\sum_{e\in E(Y)}\sqrt{\frac{d_\sigma+d_\tau-2}{d_\sigma d_\tau}}+w_i\sum_{e'\in E(Y')}\sqrt{\frac{d_\sigma+d_\tau-2}{d_\sigma d_\tau}}$
7	M_1^D	First Zagreb Index - Double	$\sum_{e\in E(Y)}(d_\sigma+d_\tau)+w_i\sum_{e'\in E(Y')}(d_\sigma+d_\tau)$
8	M_2^D	Second Modified Zagreb Index - Double	$\sum_{e\in E(Y)}\frac{1}{d_\sigma\times d_\tau}+w_i\sum_{e'\in E(Y')}\frac{1}{d_\sigma\times d_\tau}$
9	SZ^D	Second Zagreb Index - Double	$\sum_{e\in E(Y)}d_\sigma\times d_\tau+w_i\sum_{e'\in E(Y')}d_\sigma\times d_\tau$
10	SK^D	Shigehalli & Kanbur Index - Double	$\sum_{e\in E(Y)}\frac{d_\sigma+d_\tau}{2}+w_i\sum_{e'\in E(Y')}\frac{d_\sigma+d_\tau}{2}$
11	GA^D	Geometric Arithmetic Index - Double	$\sum_{e\in E(Y)}\frac{2\sqrt{d_\sigma d_\tau}}{d_\sigma+d_\tau}+w_i\sum_{e'\in E(Y')}\frac{2\sqrt{d_\sigma d_\tau}}{d_\sigma+d_\tau}$
12	R^D	Randic Index - Double	$\sum_{e\in E(Y)}\frac{1}{\sqrt{d_\sigma\times d_\tau}}+w_i\sum_{e'\in E(Y')}\frac{1}{\sqrt{d_\sigma\times d_\tau}}$
13	SO^D	Sombar Index - Double	$\sum_{e\in E(Y)}\sqrt{d_\sigma^2+d_\tau^2}+w_i\sum_{e'\in E(Y')}\sqrt{d_\sigma^2+d_\tau^2}$

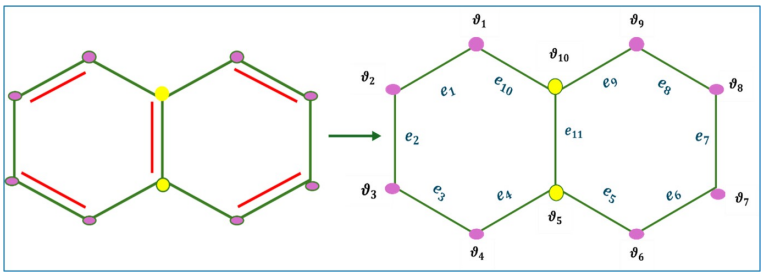

Fig. 8. :Naphthalene- molecular structure and its simple graph

The figure shows that the simple graph of naphthalene contains ten vertices and 11 edges. Hence, the duplicate graph of naphthalene contains 20 (two sets of 10) vertices placed parallel and twenty-two (two sets of 11) edges connecting the vertices. The process of assigning weights to the edges while preserving the properties of the graph is as follows. The weights for the 22 edges in the duplicate graph are assigned according to the nature of the corresponding edges in the two generated graph components, as shown. The edges are presented in three colors to better understand the idea of assigning weights. In the naphthalene graph, edges of weight zero are added between vertices where single bonds are present. The above graph does not possess the properties of a simple connected

graph. However, contains two graph components (named C1 and C2), which are simply connected graphs. The two sets of vertices ϑ_i and $\vartheta_i^{'}$ exists and $\vartheta_i = \vartheta_i^{'}$,for all $i = 1, 2 \ldots 10$. By using the vertex relations and labelling theorems, the vertices in C1 and C2 can be alternatively named. The entire process is portrayed in Figure 9.

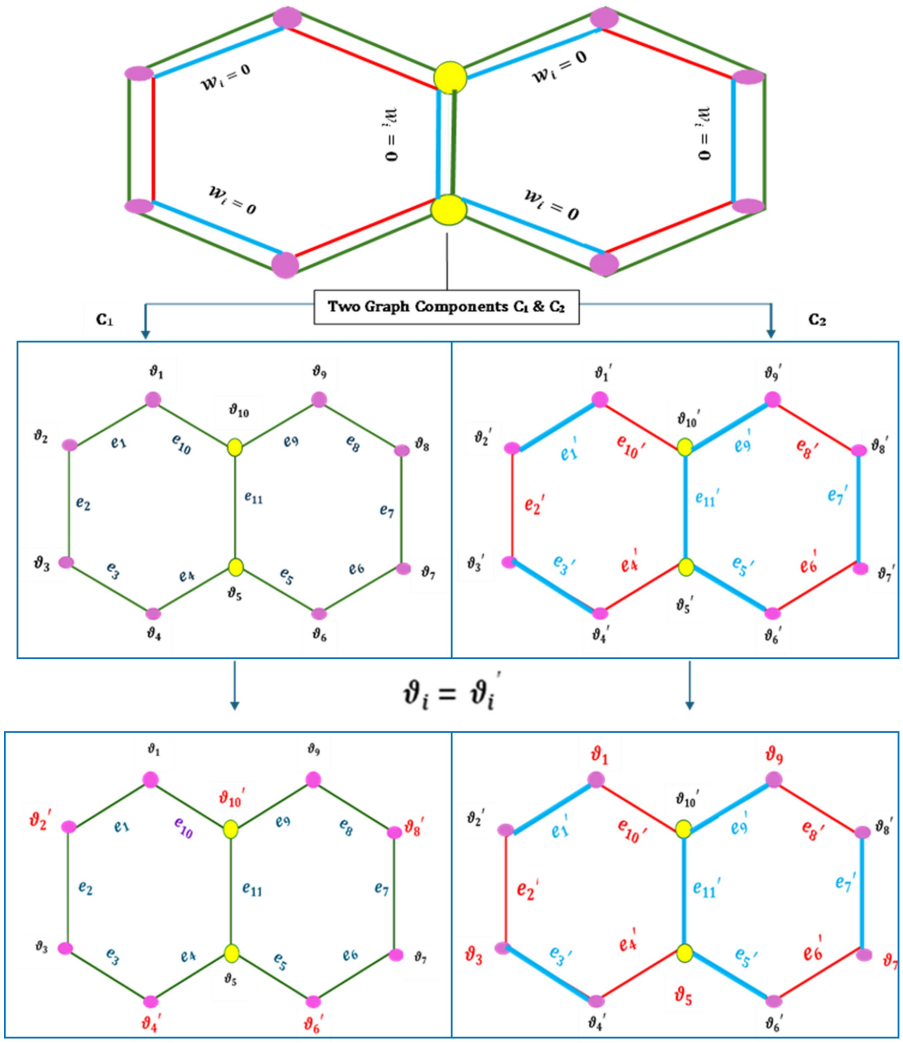

Fig. 9. Vertex & Edges of graph components corresponding to duplicate graphs

Figure 9 ensure the presence of two sets of edges e_i and $e_i^{'}$, corresponding to every edge E_i , of the simple graph. Thus, two sets of vertices and edges satisfying the conditions of duplicate graphs exists in the graph components. The edges of the duplicate graph correspond with the components' edges which enable assigning weights.

• The edges e_i of the duplicate graph correspond to the edges of the component graph C1. A unit weight is assigned to the corresponding edges e_i

•The edges $e_i^{'}$ of the duplicate graph corresponds to the edges of the component graph C2. Two different weights are assigned to the edges $e_i^{'}$

•Edges corresponding to the newly added edges are assigned a weight zero. This process nullifies the addition and preserves the molecular structure. Remaining edges which correspond to the double bond are assigned weight θ_i. The duplicate graph of the simple graph of Naphthalene is portrayed in Figure 10.

The vertices $\vartheta_5, \vartheta_{10}, \vartheta_5^{'}, \vartheta_{10}^{'}$ are of degree 3 according to the sum of edges incident on it. Remaining

vertices occur with degree 2. The details of edges and weights are in Table 3.

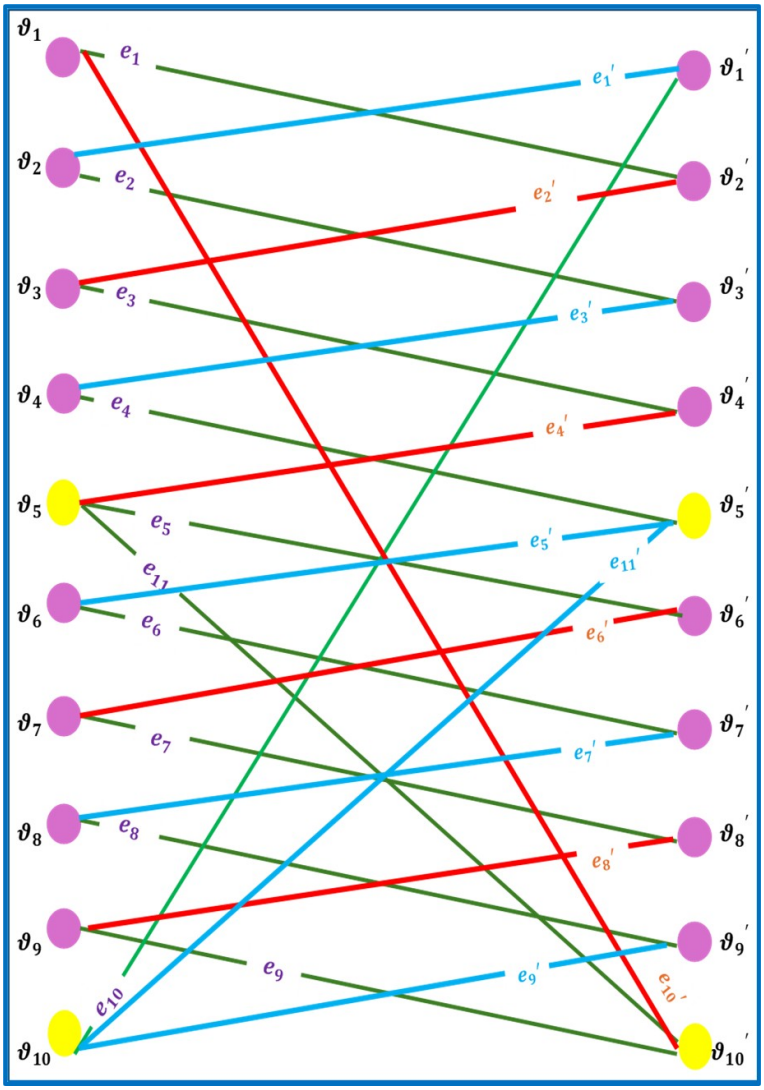

Fig. 10. Duplicate graph of Naphthalene

From the Table 3, it is evident that the total number of edges with non-zero weights is 16. Hence N=16. The edge set of the duplicate graph (naphthalene) possesses the partitions:

$$
\begin{aligned}
E_1(\mathfrak{G}) =& E_{22} = \{\partial \in E_1(\mathfrak{G}) : d_\alpha(\mathfrak{G}) = 2 \text{ and } d_\beta(\mathfrak{G}) = 2\},\\
E_2(\mathfrak{G}) =& E_{23} = \{\partial \in E_1\mathfrak{G} : d_\alpha(\mathfrak{G}) = 2 \text{ and } d_\beta(\mathfrak{G}) = 3\},\\
E_3(\mathfrak{G}) =& E_{33} = \{\partial \in E_1(\mathfrak{G}) : d_\alpha(\mathfrak{G}) = 3 \text{ and } d_\beta(\mathfrak{G}) = 3\},\\
E_1(\mathfrak{G}') =& E_{22} = \{\partial' \in E_1(\mathfrak{G}') : d_\alpha(\mathfrak{G}') = 2 \text{ and } d_\beta(\mathfrak{G}') = 2\},\\
E_2(\mathfrak{G}') =& E_{23} = \{\partial' \in E_1(\mathfrak{G}') : d_\alpha(\mathfrak{G}') = 2 \text{ and } d_\beta(\mathfrak{G}') = 3\},\\
E_3(\mathfrak{G}') =& E_{33} = \{\partial' \in E_1(\mathfrak{G}') : d_\alpha(\mathfrak{G}') = 3 \text{ and } d_\beta(\mathfrak{G}') = 3\}.
\end{aligned}
$$

The cardinality of each partition is listed in Table 4.

Thus, sum of cardinalities of E is 11,and sum of cardinalities of E' is 5 yielding N=16. Hence, $\theta_i = \frac{\tau_i}{N} = \frac{3}{16}, \frac{2}{16}, \frac{0}{16}$. It is evident that, number of bonds in molecular structure of naphthalene and edge cardinality are equal. This ensures that new degree-based TIs preserve the molecular structure.

Table 3. Edge representations with corresponding weight (Naphthalene - Duplicate Graph)

S.No	E	Representation	w_i	E'	Representation	w_i
1	e_1		1	e'_1		θ_i
2	e_2		1	e'_2		0
3	e_3		1	e'_3		θ_i
4	e_4		1	e'_4		0
5	e_5		1	e'_5		θ_i
6	e_6		1	e'_6		0
7	e_7		1	e'_7		θ_i
8	e_8		1	e'_8		0
9	e_9		1	e'_9		θ_i
10	e_{10}		1	e'_{10}		0
11	e_{11}		1	e'_{11}		θ_i

Table 4. Edge Partition cardinality of Naphthalene

S.No	Cardinality of E	Cardinality of E'
1	$E(2,2) = 6$	$E'(2,2) = 3$
2	$E(2,3) = 4$	$E'(2,3) = 2$
3	$E(3,3) = 1$	$E'(3,3) = 0$
Sum	$\sum E = 11$	$\sum E' = 5$

The structure of PAHs along with θ_i values of $E'(2,2), E'(2,3), E'(3,3)$ partitions are presented in Table 5.

Table 5. Molecular Structure of PAHs considered for study

1. Naphthalene 	2. Acenaphthylene 	3. Acenaphthene 	4. Fluorene 
$\theta_i = \frac{3}{16}, \frac{2}{16}, \frac{0}{16}$	$\theta_i = \frac{3}{20}, \frac{2}{20}, \frac{1}{20}$	$\theta_i = \frac{2}{19}, \frac{2}{19}, \frac{1}{19}$	$\theta_i = \frac{4}{21}, \frac{0}{21}, \frac{2}{21}$
5. Phenanthrene 	6. Fluoranthene 	7. Benz(a) anthracene 	8. Benzo(b) fluoranthene 
$\theta_i = \frac{5}{23}, \frac{0}{23}, \frac{2}{23}$	$\theta_i = \frac{4}{27}, \frac{2}{27}, \frac{2}{27}$	$\theta_i = \frac{4}{30}, \frac{4}{30}, \frac{1}{30}$	$\theta_i = \frac{3}{33}, \frac{6}{33}, \frac{1}{33}$
9. Indeno (1,2,3-cd) pyrene 	10. Acephenanthrylene 	11. Benzo[j] fluoranthene 	12. Benzo[ghi] fluoranthene 
$\theta_i = \frac{2}{37}, \frac{7}{37}, \frac{2}{37}$	$\theta_i = \frac{4}{27}, \frac{4}{27}, \frac{2}{27}$	$\theta_i = \frac{5}{34}, \frac{2}{34}, \frac{3}{34}$	$\theta_i = \frac{3}{31}, \frac{4}{31}, \frac{2}{31}$
13. Benzo[b] triphenylene 	14. Dibenz[a,h] acridine 	15. Coronene 	16. Dibenzo [b,def]chrysene 
$\theta_i = \frac{3}{37}, \frac{8}{37}, \frac{0}{37}$	$\theta_i = \frac{4}{37}, \frac{6}{37}, \frac{1}{37}$	$\theta_i = \frac{3}{42}, \frac{6}{42}, \frac{3}{42}$	$\theta_i = \frac{4}{41}, \frac{6}{41}, \frac{2}{41}$

The physiochemical properties of the PAHs obtained from the recognized databases and the predicted values using double-bond TIs are presented in Tables 6 to 9.

Table 6. Chemical Properties of Various Compounds

S.No	Chemical/ Property	BP (°C)	EV (kJ/mol)	FP (°C)	IR	Pol	MV (cm^3/ mol)	ST (mN/ m)
1	Naphthalene	221.5	43.9	78.9	1.632	17.5	123.5	40.2
2	Acenaphthylene	298.9	51.7	137.2	1.732	20.3	128.2	54.7
3	Acenaphthene	279.0	49.7	135.3	1.692	20.5	134.9	49.2
4	Fluorene	293.6	51.2	133.1	1.645	21.3	148.3	46.2
5	Phenanthrene	337.4	55.8	146.6	1.715	24.6	157.7	48.0
6	Fluoranthene	375.0	59.8	168.4	1.852	28.7	162.0	59.4
7	Benz(a) anthracene	436.7	66.7	209.1	1.771	31.6	191.8	53.5
8	Benzo(b) fluoranthene	467.5	70.2	228.6	1.887	35.8	196.1	63.5
9	Indeno (1,2,3-cd)pyrene	497.1	73.6	247.2	2.009	40.0	200.0	74.2
10	Acephenan -thrylene	405.7	63.2	188.6	1.796	27.4	162.3	60.4
11	Benzo[j] fluoranthene	467.5	70.2	228.6	1.887	35.8	196.1	63.5
12	Benzo[ghi] fluoranthene	406.0	63.2	189.9	1.997	32.9	166.3	72.0
13	Benzo[b] triphenylene	518.0	76.1	264.5	1.812	38.7	225.9	57.7
14	Dibenz[a,h] acridine	534.0	78.0	240.3	1.824	37.9	219.1	62.8
15	Coronene	525.6	77.0	265.2	2.140	44.1	204.7	85.8
16	Dibenzo [b,def] chrysene	552.3	80.2	282.0	1.913	42.9	230.2	66.5

Table 7. Physio-chemical properties of PAHs

S.No	Chemical/Property	MM	RI	MW	XlogP3-AA	HAC	Complexity	LogP
1	Naphthalene	128.062	200	128.17	3.3	10	80.6	3.35
2	Acenaphthylene	152.192	244	152.19	3.7	12	184	3.93
3	Acenaphthene	154.078	247.8	154.21	3.9	12	155	3.9
4	Fluorene	166.0782	270.8	166.22	4.2	13	165	4.8
5	Phenanthrene	178.078	300	178.23	4.5	14	174	4.46
6	Fluoranthene	202.078	300	202.26	5.2	16	243	5.16
7	Benz(a)anthracene	228.0939	400	228.3	5.8	18	294	5.76
8	Benzo(b)fluoranthene	252.094	442.1	252.3	6.4	20	372	5.78
9	Indeno(1,2,3-cd)pyrene	276.0939	495.3	276.3	7.0	22	453	6.58
10	Acephenanthrylene	202.078	348.14	202.25	4.9	16	303	—
11	Benzo[j]fluoranthene	252.0939	443	252.3	6.4	20	372	—
12	Benzo[ghi]fluoranthene	226.078	391.6	226.3	5.4	18	314	7.23
13	Benzo[b]triphenylene	278.1095	495.9	278.3	6.7	22	361	—
14	Dibenz[a,h]acridine	279.1047	488.55	279.3	6.0	22	405	5.73
15	Coronene	300.352	593.5	300.4	7.2	24	376	—
16	Dibenzo[b,def]chrysene	302.1095	559.9	302.4	7.0	24	436	—

Table 8. Double bond TIs of PAHs

S.No	Chemical/TI	ISD	M2RD	$M2RD^D$	SDD^D	SC^D	$M1^D$	ABC^D
1	Naphthalene	13.74	10.51	12.196	26.322	5.323	51.2	7.926
2	Acenaphthylene	18.395	13.18	15.671	34.192	6.548	69.4	9.988
3	Acenaphthene	18.2211	13.14	15.635	34.123	6.529	69.2632	9.962
4	Fluorene	19.6429	14.15	16.677	36.246	7.041	73.3333	10.69
5	Phenanthrene	20.613	15.2	17.653	38.109	7.552	77.3913	11.4
6	Fluoranthene	25.437	18.18	20.661	44.16	8.77	95.4074	13.4
7	Benzo(a)anthracene	28.5667	19.45	23.562	51.828	9.745	103.4	14.9
8	Benzo(b)fluoranthene	31.2121	22.01	24.89	53.078	10.54	116.455	16.15
9	Indeno(1,2,3-cd)pyrene	37.1351	25.41	29.554	63.856	12.18	139.351	18.88
10	Acephenanthrylene	25.25556	17.815	21.1109	45.9938	8.7564	95.4074	13.439
11	Benzo[j]fluoranthene	32.37647	22.805	26.1185	56.0294	10.979	121.412	16.853
12	Benzo[ghi]fluoranthene	30.19355	20.799	24.1173	52.0323	9.9761	113.419	15.436
13	Benzo[b]triphenylene	33.17143	23.414	27.5781	59.9214	11.554	123.343	17.637
14	Dibenz[a,h]acridine	34.52432	24.075	29.0185	63.6937	11.954	129.405	18.35
15	Coronene	41.8286	28.08	32.983	71.571	13.4	157.429	20.92
16	Dibenzo[b,def]chrysene	39.09024	27.082	32.0006	69.6301	13.176	147.415	20.345

Table 9. Double bond TIs of PAHs

S.No	Chemical/TI	$M2D^D$	SZD^D	SKD^D	GAD^D	RD^D	SOD^D
1	Naphthalene	2.333	58.33	25.6	11.18	5.08743	36.49327
2	Acenaphthylene	2.643	84.65	34.7	14.2	6.08198	49.50032
3	Acenaphthene	2.633	84.53	34.63158	14.1	6.06264	49.40392
4	Fluorene	2.889	88.52	36.66667	15.2	6.57487	52.28794
5	Phenanthrene	3.147	92.65	38.69565	16.2	7.08717	55.14402
6	Fluoranthene	3.474	119.7	47.7037	19.2	8.0785	67.88852
7	Benzo(a)anthracene	3.921	125.7	51.7	21.1	9.04859	73.81968
8	Benzo(b)fluoranthene	4.114	147.8	58.22727	23.2	9.65521	82.84016
9	Indeno(1,2,3-cd)pyrene	4.574	179.7	69.67568	27.06	11.02706	99.24781
10	Acephenanthrylene	3.4465	118.7	47.7037	19.13	8.061659	68.02855
11	Benzo[j]fluoranthene	4.2778	153.71	60.70588	24.13	10.05911	86.41946
12	Benzo[ghi]fluoranthene	3.7751	145.74	56.70968	22.13	9.055223	80.76877
13	Benzo[b]triphenylene	4.6381	151.54	61.67143	25.08	10.70699	87.93075
14	Dibenz[a,h]acridine	4.7245	159.68	64.7027	26.05	11.0287	92.35122
15	Coronene	4.885	205.9	78.71429	30	12.018	112.159
16	Dibenzo[b,def]chrysene	5.0556	186.76	73.70732	29.05	12.02459	105.0815

2.2. Regression models

Quantifying the relationship between the properties of any chemical compound and the corresponding TIs is an essential element of QSPR investigation [50]. Regression analysis and modelling is used as a tool in QSPR investigations to accurately predict or estimate the properties of any compound using TIs [49]. The predictions derived from the double-bond TIs (Tables 8 and 9) are correlated with the physicochemical property values(Tables 6 and 7) of the considered PAHs. The linear and quadratic models of regression further confirmed this association, as good correlation values were obtained. The TIs obtained for the molecular structures of PAHs were regarded as independent variables, and the physicochemical attributes were designated as dependent variables [33]. The quadratic and linear regression models are given by the following equation, respectively

$$pc = \mathcal{F}_1(TI) + S, \tag{1}$$

$$pc = \mathcal{F}_1(TI)^2 + \mathcal{F}_2(TI) + S, \tag{2}$$

where pc denotes the physio-chemical property, S is the intercept (constant), $\mathcal{F}_1$ and $\mathcal{F}_2$ denote the regression coefficients (constants). QSPR model's accuracy is determined by investigating its correlation coefficient (r^2). As per the guidelines of the International Academy of Mathematical Chemistry, a quality QSPR model should have $r^2 > 0.8$. The best prediction model is the one with the lowest RMSE, or the least amount of error. F-statistics is used to evaluate the model's quality of fit [7, 18]. In the regression model, any trait with a p-value larger than 0.05 and a correlation greater than 0.6 is deemed significant [27].

2.3. Linear regression analysis

Linear regression models were created using the set of 13 TIs for each physicochemical property using Eq. (1). For the physiochemical characteristics described above that correlate with the double bond indices, the corresponding intercepts and constants were calculated. F-statistics were used to test linear regression models. The best prediction models were provided by the five recently proposed TIs. The following are the best predictions obtained using this model:

- M_2^D Index predicts BP, EV, FP, and MV with r^2 values of 0.9811, 0.984, 0.9626, and 0.9494 respectively.
- SZ^D index predicts IR, ST, MP whose r^2 values are +0.898527, 0.82055, and 0.716 respectively.
- M^2R^D predicts Log P, Polarization, X-Log P3 AA with r^2 values of 0.9366, 0.99312, and 0.9573 respectively.
- R^D predicts MM, MW, HAC and can be predicted with r^2 values of 0.99653, 0.9965, and 0.9972 respectively.
- M^2RDD^D predicts RI with an r^2 value of 0.9804.
- SC^D predicts complexity with an r^2 value of 0.91556.The best predictive linear regression models obtained from Eq. (1) are as follows:

$$\begin{aligned} BP &= 116.58M_2^D - 27.553, \\ EV &= 12.894M_2^D + 15.627, \\ FP &= 65.638M_2^D - 51.856, \\ MV &= 38.397M_2^D + 32.679, \end{aligned}$$

$$
\begin{aligned}
MM &= 25.336R^D - 0.7675,\\
MW &= 25.352R^D - 0.7395,\\
HAC &= 2.044R^D - 0.4097,\\
IR &= 0.003SZ^D + 1.4407,\\
LogP &= 0.2288M_2R^D + 1.1588,\\
Polar &= 1.5952M_2R^D + 0.1849,\\
X\ Log\ P3\ AA &= 0.233M_2R^D + 0.884,\\
COMP &= 42.974SZ^D - 120.69,\\
ST &= 0.2491SZ^D + 27.099,\\
MP &= 1.878SZ^D - 73.422,\\
RI &= 18.895M_2^D - 47.489.
\end{aligned}
$$

The statistical parameters of the best-fit linear regression model are listed in Table 10. The results obtained for the quadratic regression models are presented graphically in Figure 11 to Figure 25.

Table 10. Statistical Parameters of the Linear regression models of PAHs

S.No	Property	TI	r	r^2	RMSE	F	p-Value
1	BP	M_2^D	0.9905	0.98115	14.7003	728.647	1.79E-13
2	EV	M_2^D	0.992	0.98406	1.49266	864.5014	5.51E-14
3	FP	M_2^D	0.9811	0.96256	11.77642	359.9385	2.2E-11
4	IR	SZ^D	0.8985	0.8070	0.06318	58.67078	2.26E-06
5	Log P	M_2R^D	0.9678	0.9366	0.3317	206.843	8.87E-10
6	PO	M_2R^D	0.9965	0.99312	0.76674	937.955	8.82E-15
7	ST	SZ^D	0.9058	0.82055	5.0692	64.01541	1.37E-06
8	MV	M_2^D	0.9744	0.9494	8.0648	262.6252	1.82E-10
9	MM	R^D	0.9983	0.99652	3.4463	4017.393	1.28E-18
10	MP	SZ^D	0.8462	0.716	56.7147	27.7373	0.000266
11	RI	M_2RD^D	0.9902	0.98049	17.4164	703.6756	2.27E-13
12	MW	R^D	0.9982	0.99651	3.4568	3997.824	1.32E-18
13	X Log P	M_2R^D	0.97844	0.9573	0.2736	314.2205	5.48E-11
14	HAC	R^D	0.99858	0.99717	0.2507	4941.147	3.01E-19
15	Complexity	SC^D	0.9568	0.91556	34.04815	151.8049	6.66E-09

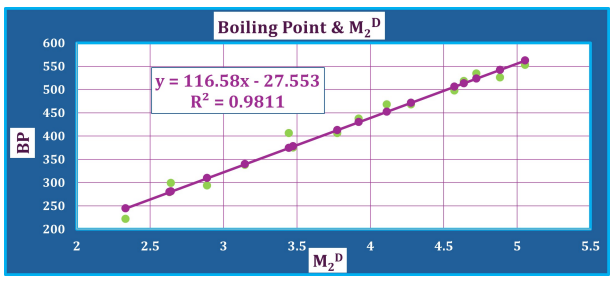

Fig. 11. Linear regression of BP &M_2^D

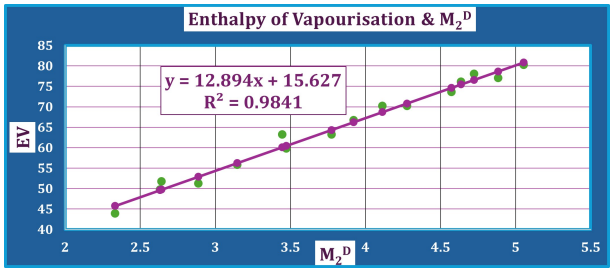

Fig. 12. Linear regression of EV &M_2^D

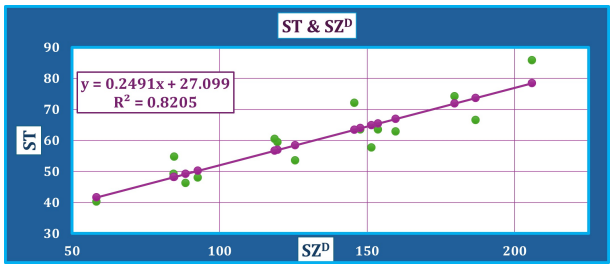

Fig. 13. Linear regression of ST &SZ^D

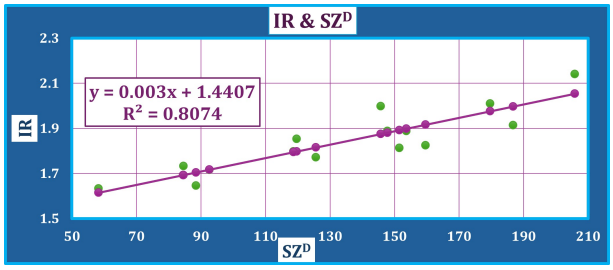

Fig. 14. Linear regression of IR &SZ^D

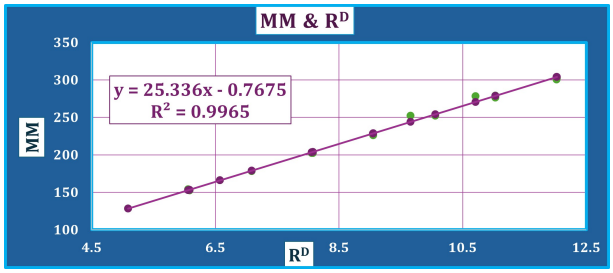

Fig. 15. Linear regression of MM &R^D

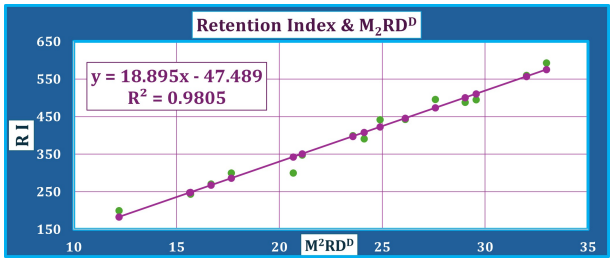

Fig. 16. Linear regression of RI &M_2R^D

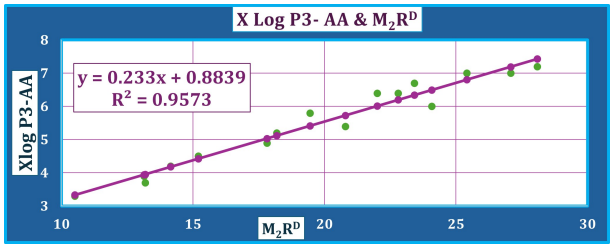

Fig. 17. Linear regression of XLog P3-AA $\&M_2R^D$

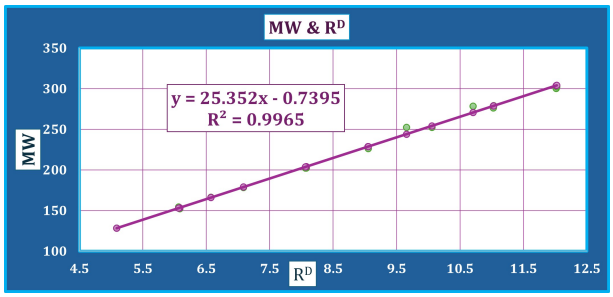

Fig. 18. Linear regression of MW $\&R^D$

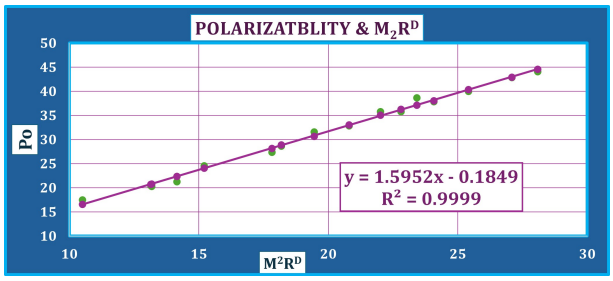

Fig. 19. Linear regression of Polarizability $\&M_2R^D$

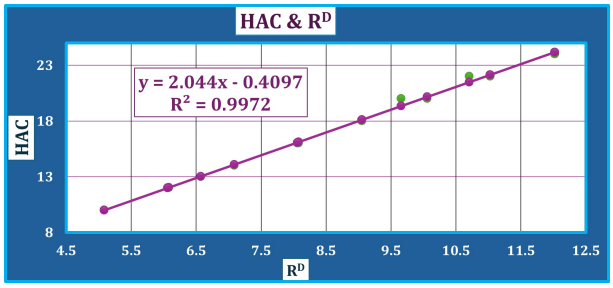

Fig. 20. Linear regression of HAC $\&R^D$

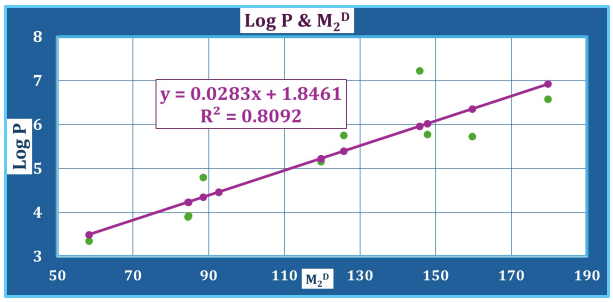

Fig. 21. Linear regression of Log P $\&M_2^D$

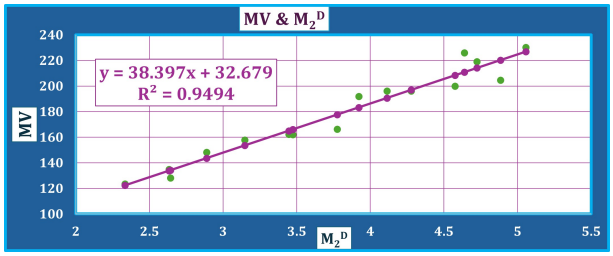

Fig. 22. Linear regression of MV $\& M_2^D$

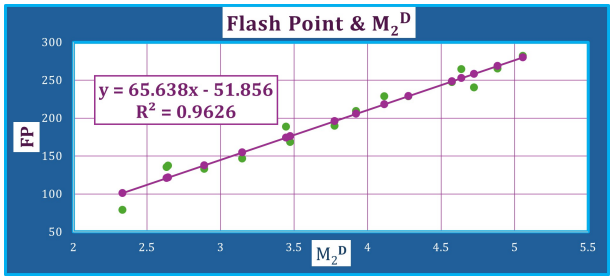

Fig. 23. Linear regression of FP $\& M_2^D$

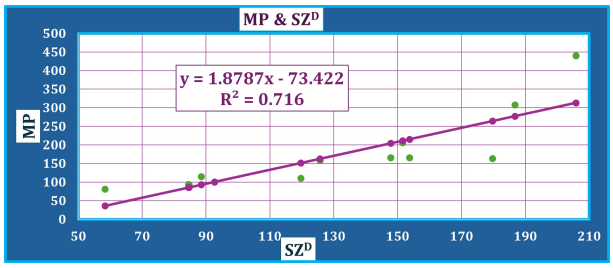

Fig. 24. Linear regression of MP $\& SZ^D$

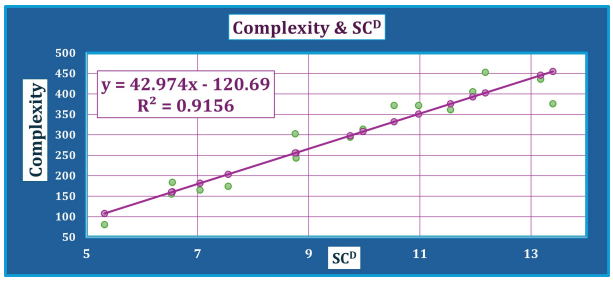

Fig. 25. Linear regression of Complexity $\& SC^D$

2.4. *Quadratic regression analysis*

Quadratic models were also created with 13 double-bond indices for the aforementioned properties. Only three TIs provided the best predictions for physicochemical properties in this model. They are

- BP can be predicted using R^D, whose r^2 value is 0.9788.
- FP can be predicted using SZ^D, whose r^2 value is 0.93173.
- EV can be predicted using SDD^D with the corresponding r^2 value 0.968705.

The best predictive Quadratic regression models obtained from Eq. (2) are:

$$BP = -2.1585(R^D)^2 + 83.373R^D - 145.44,$$
$$FP = -0.0053(SZ^D)^2 + 2.7355SZ^D - 62.602,$$

$$EV = -0.0069(SDD^D)^2 + 1.50354SDD^D + 7.7553.$$

The best-fit quadratic regression model and parameters (statistical) are listed in Table 11, and their corresponding visualizations are shown in Figures 26 to 28.

Table 11. Statistical Parameters of Quadratic regression model of PAHs

S.No	Property	TI	r	r^2	RMSE	F	p-Value
1	BP	R^D	0.98936	0.97884	16.1622	300.6883	1.31E-11
2	FP	SZ^D	0.9653	0.93173	16.50276	88.7102	2.65E-08
3	EV	SDD^D	0.98423	0.968705	2.1706	201.2	1.66E-10

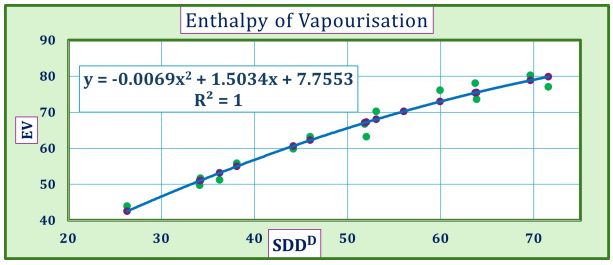

Fig. 26. Quadratic regression of EV &SDD^D

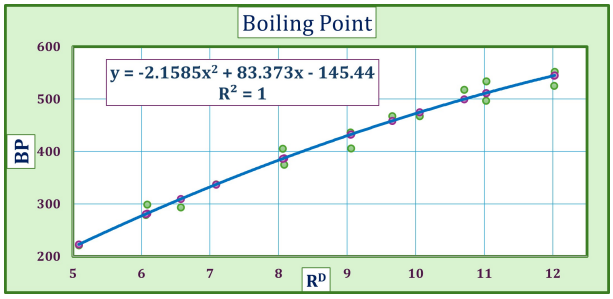

Fig. 27. Quadratic regression of BP &R^D

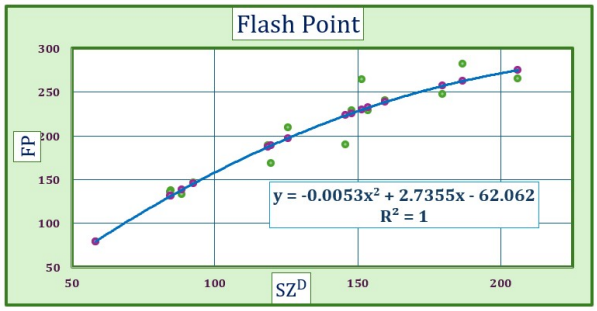

Fig. 28. Quadratic regression of FP &SZ^D

Thus, best-fit linear and quadratic regression models were developed for PAHs using double bond indices. Widely used degree-based indices have been extended to double-bond indices. The new indices show stronger, and sometimes marginally weaker, correlations with various properties than the former ones. Hence, to ensure the efficiency of these indices, their results must be compared to those of existing indices. Therefore, an intercorrelation matrix and sensitivity analysis were used. The values of the existing TIs of the PAHs are presented in Tables 12 and 13.

Table 12. Numerals of PAHs evaluated for existing degree-based indices

S.No	Chemical/TI	IS	M2R	M2RD	SDD	SC	ABC	M1
1	Naphthalene	12.3	10.266	11.899	25.667	5.197	7.737	50
2	Acenaphthylene	16.7	12.898	15.348	33.5	6.408	9.778	68
3	Acenaphthene	16.7	12.898	15.348	33.5	6.408	9.778	68
4	Fluorene	17.7	13.899	16.348	35.5	6.908	10.485	73.333
5	Phenanthrene	18.7	14.899	17.348	37.5	7.408	11.192	77.391
6	Fluoranthene	23.2	17.899	20.348	43.5	8.633	13.399	94
7	Benzo(a)anthracene	25	19.165	23.247	51.167	9.605	14.687	102
8	Benzo(b)fluoranthene	28.4	21.715	24.573	52.416	10.396	15.939	115
9	Indeno(1,2,3-cd)pyrene	34	25.165	29.247	63.167	12.054	18.687	138
10	Acephenanthrylene	23.1	17.532	20.798	45.333	8.618	13.233	94
11	Benzo[j]fluoranthene	29.6	22.532	25.798	55.333	10.844	16.647	120
12	Benzo[ghi]fluoranthene	27.6	20.532	23.798	51.333	9.844	15.233	112
13	Benzo[b]triphenylene	30	23.165	27.247	59.167	11.422	17.435	122
14	Dibenz[a,h]acridine	31.4	23.798	23.697	63	11.816	18.142	128
15	Coronene	38.4	27.798	32.697	71	12.265	20.728	156
16	Dibenzo[b,def]chrysene	35.9	26.798	31.697	69	13.041	20.142	146

Table 13. Numerals of PAHs evaluated for existing degree-based indices

S.No	Chemical/TI	SZ	M2	SK	GA	R	SO
1	Naphthalene	2.277	57	25	10.919	4.966	35.635
2	Acenaphthylene	2.5833	83	34	13.878	5.949	48.503
3	Acenaphthene	2.5833	83	34	13.878	5.949	48.503
4	Fluorene	2.8333	87	36	14.878	6.449	51.332
5	Phenanthrene	3.0833	91	38	15.878	6.949	54.16
6	Fluoranthene	3.1466	118	47	18.878	7.949	66.888
7	Benzo(a)anthracene	3.8611	124	51	20.797	8.915	72.825
8	Benzo(b)fluoranthene	4.0555	146	57.5	22.858	9.524	81.807
9	Indeno(1,2,3-cd)pyrene	4.528	178	69	29.797	10.915	98.28
10	Acephenanthrylene	3.388	117	47	18.838	7.933	67.028
11	Benzo[j]fluoranthene	4.222	152	60	23.838	9.932	85.413
12	Benzo[ghi]fluoranthene	3.722	144	56	18.878	8.933	79.756
13	Benzo[b]triphenylene	4.583	150	61	24.797	10.852	86.967
14	Dibenz[a,h]acridine	4.667	158	64	25.757	10.898	91.349
15	Coronene	4.833	204	78	29.757	11.898	111.15
16	Dibenzo[b,def]chrysene	5	185	73	28.757	11.898	104.08

2.5. Intercorrelation matrix

An intercorrelation matrix can be used to quantify the behavior of the indices. The correlation coefficient, r, was used to frame the matrix. It is evident from the table that all the r values lie

between $1 \geq r \geq 0.96$. There is a substantial connection between the pairs of TIs whose $r \geq 0.98$. Table 15 presents an intercorrelation matrix framed between the suggested new indices and current indices. Consequently, the new indices that have been expanded show remarkable connections with the degree-based topological indices examined. Therefore, the use of current indices to anticipate the physicochemical features of double-bond TIs is equally likely.

2.6. Sensitivity analysis

The phenomenon in which two or more distinct chemical structures have the same TI value at times is known as TIs' degeneracy. The predictive capacity of TIs is constrained by reduced discriminative power. The analysis introduced by Konstantinova was used to quantitatively measure the degeneracy sensitivity [61], which is defined as follows:

$$S = \frac{\mathfrak{N}}{\mathfrak{N}_k - \mathfrak{N}},$$

where, $\mathfrak{N}$ and $\mathfrak{N}$ represents the number of molecular structures under study and the undistinguished numbers in each TI respectively. The discriminatory potential of a given TI was quantified based on its level of degeneracy. High-discriminating-power TIs frequently capture additional structural information. As S rises, TIs' capacity for discrimination grows. A comparative sensitivity analysis between the double-bond degree-based TIs and existing TIs is presented in Table 14.

Table 14. Sensitivity analysis of topological indices

S.No	TI-Double	Sensitivity Analysis	TI	Sensitivity Analysis
1	ISD^D	1	IS	0.875
2	$M2R^D$	1	M2R	0.875
3	$M2RD^D$	1	M2RD	0.875
4	SDD^D	1	SDD	0.875
5	SC^D	1	SC	0.875
6	ABC^D	1	ABC	0.875
7	$M1^D$	1	M1	0.75
8	$M2^D$	1	M2	0.875
9	SZ^D	1	SZ	0.875
10	SK^D	1	SK	0.875
11	GA^D	1	GA	0.75
12	R^D	1	R	0.75
13	SO^D	1	SO	0.875

The tabular data unequivocally demonstrates that each double-bond index possesses a 100% discriminative potential. Consequently, the expanded indices exhibit superior discriminating capabilities in comparison to traditional topological indices (TIs).

2.7. Highlights and prospects

This investigation's results provide a foundation for enhancing the accuracy of physicochemical property predictions in polycyclic aromatic hydrocarbons (PAHs). The naphthalene representation effectively maintains both the structural attributes of the chemical compound and the mathematical

characteristics of the simple connected graph. The intercorrelation matrix and sensitivity analysis validate the extended double-bond indices' predictive capacity and comprehensive discriminative power. Table 16 encapsulates the primary points evaluated within the same table.

Table 15. Intercorrelation matrix between double bond indices and existing Topological Indices

TIs	IS^D	IS	M^2R^D	M^2R	M^2RD^D	M^2RD	SDD^D	SDD	SC^D	SC	ABC^D	ABC	M_1^D	M_1	M_2^D	M_2	SZ^D	SZ	SK^D	SK	GA^D	GA	R^D	R	SO^D	SO
IS^D	1																									
IS	0.999	1																								
M^2R^D	0.998	0.998	1																							
M^2R	0.998	0.998	1	1																						
M^2RD^D	0.997	0.996	0.997	0.997	1																					
M^2RD	0.986	0.986	0.984	0.984	0.980	1																				
SDD^D	0.995	0.993	0.994	0.994	0.999	0.977	1																			
SDD	0.995	0.993	0.994	0.994	0.999	0.977	1	1																		
SC^D	0.996	0.995	0.998	0.998	0.999	0.980	0.998	0.998	1																	
SC	0.987	0.985	0.992	0.992	0.993	0.970	0.991	0.991	0.996	1																
ABC^D	0.998	0.997	0.999	0.999	1	0.982	0.998	0.998	1	0.994	1															
ABC	0.998	0.997	0.999	0.999	0.999	0.982	0.998	0.998	1	0.994	1	1														
M_1^D	0.999	1	0.998	0.998	0.996	0.985	0.994	0.994	0.995	0.986	0.997	0.997	1													
M_1	0.999	1	0.998	0.998	0.996	0.985	0.994	0.994	0.995	0.986	0.997	0.997	1	1												
M_2^D	0.981	0.977	0.987	0.987	0.990	0.962	0.989	0.989	0.993	0.995	0.990	0.990	0.977	0.978	1											
M_2	0.978	0.974	0.983	0.983	0.988	0.960	0.988	.988	0.991	0.992	0.988	0.987	0.975	0.975	0.997	1										
SZ^D	0.997	0.998	0.994	0.994	0.990	0.984	0.986	0.986	0.988	0.976	0.991	0.991	0.998	0.998	0.964	0.960	1									
SZ	0.997	0.999	0.994	0.994	0.990	0.984	0.986	0.987	0.988	0.976	0.991	0.991	0.998	0.998	0.964	0.961	1	1								
SK^p	0.999	1	0.998	0.998	0.996	0.985	0.994	0.994	0.995	0.986	0.997	0.997	1	1	0.977	0.975	0.998	0.998	1							
SK	0.999	1	0.998	0.998	0.996	0.985	0.994	0.994	0.995	0.986	0.997	0.997	1.000	1	0.977	0.975	0.998	0.998	1	1						
GA^p	0.999	0.998	1	1	0.999	0.983	0.997	0.997	0.999	0.993	1.000	1	0.998	0.998	0.989	0.986	0.993	0.993	0.998	0.998	1					
GA	0.982	0.981	0.983	0.983	0983	0.969	0.981	0.981	0.984	0.979	0.984	0.984	0.981	0.981	0.974	0.972	0.975	0.975	0.981	0.981	0.984	1				
R^D	0.993	0.990	0.996	0.996	0.998	0.975	0.996	0.996	0.999	0.997	0.998	0.998	0.991	0.991	0.997	0.994	0.981	0.982	0.991	0.991	0.997	0.982	1			
R	0.991	0.988	0.995	0.995	0.996	0.975	0.995	0.995	0.998	0.996	0.997	0.997	0.989	0.989	0.998	0.995	0.979	0.979	0.989	0.989	0.996	0.981	1	1		
$S0^D$	0.999	1	0.998	0.998	0.997	0.985	0.994	0.994	0.995	0.986	0.997	0.997	1	1	0.978	0.975	0.998	0.998	1	1	0.998	0.981	0.991	0.989	1	
$S0$	0.999	1	0.998	0.998	0.997	0.985	0.994	0.994	0.995	0.986	0.997	0.997	1	1	0.978	0.975	0.998	0.998	1	1	0.998	0.981	0.991	0.989	1	1

Table 16. Highlights of the Extended TIs

Topological Indices	Extended Topological Indices
Neglect to detect double bonding	Double bonds are recognized
Less discriminating power	Higher discriminating power
Chemical undergoes structural modification	Structure of the compound is not modified

These promising results lead to many futures works especially,

- Adding various bond kinds namely, triple bonds to the indexes.
- Forecasting and verifying other sets of chemical structures.
- To lessen the degeneracy of various degree-based indices the formulations can be extended .
- Large network graph TI prediction is made easier by coding them in a programming language and incorporating them into a software package.

More than 500,000 chemical entities are synthesized and characterized annually [11]. The prediction of biological activity in molecular structures is paramount for enhancing therapeutic efficacy and mitigating adverse effects, including toxicity. While traditional experimental methods for determining physicochemical properties are resource-intensive and costly, topological indices (TIs) offer a more economical approach. These indices serve as valuable tools in optimizing the therapeutic index of lead compounds, thereby streamlining the drug development process.

3. Conclusion

The indices examined in this study demonstrate robust predictive capabilities for physicochemical properties, significantly enhancing the virtual screening process of PAHs. Notable accomplishments of this research include improved discriminatory power and the preservation of double-bonded molecular structures. Expanding this concept to diverse molecular structures could substantially broaden the

scope and impact of this investigation. The findings presented herein are expected to make significant contributions to QSAR/QSPR studies, ultimately increasing the practical utility of TIs in the virtual screening of lead compounds within pharmaceutical sciences.

Declaration of interest

The authors do not declare any conflicting interest. The writers alone are in charge of the composition and contents of this work.

References

[1] D. Alghazzawi, A. Raza, U. Munir, and M. Ali. Chemical applicability of newly introduced topological invariants and their relation with polycyclic compounds. *Journal of Mathematics*, 2022:5867040, 2022. https://doi.org/10.1155/2022/5867040.

[2] D. Anuradha and B. Jaganathan. Topological properties of boron triangular sheet for robotic finger flex motion through indices. *AIP Conference and Proceeding*, 2946:020013, 2023. https://doi.org/10.1063/5.0178070.

[3] D. Anuradha, K. Julietraja, B. Jaganathan, and A. Alsinai. Curcumin-conjugated pamam dendrimers of two generations: comparative analysis of physiochemical properties using adriatic topological indices. *ACS Omega*, 9(12):14558–14579, 2024. https://doi.org/10.1021/acsomega.4c00686.

[4] D. Balasubramaniyan and N. Chidambaram. On some neighbourhood degree-based topological indices with qspr analysis of asthma drugs. *The European Physical Journal Plus*, 138:823, 2023. https://doi.org/10.1140/epjp/s13360-023-04439-7.

[5] M. Chauhan, J. Buragohain, A. Bharali, and M. Essa Nazari. Predictive ability of neighborhood degree sum-based topological indices of polycyclic aromatic hydrocarbons. *Journal of Molecular Structure*, 1270:133904, 2022. https://doi.org/10.1016/j.molstruc.2022.133904.

[6] D. Ciubotariu, M. Medeleanu, V. Vlaia, T. Olariu, C. Ciubotariu, D. Dragos, and S. Corina. Molecular van der waals space and topological indices from the distance matrix. *Molecules*, 9(12):1053–1078, 2004. https://doi.org/10.3390/91201053.

[7] O. Colakoglu. Qspr modeling with topological indices of some potential drug candidates against covid-19. *Journal of Mathematics*, 2022:3785932, 2022. https://doi.org/10.1155/2022/3785932.

[8] R. Cruz, J. Monsalve, and J. Rada. Randić energy of digraphs. *Heliyon*, 8(11):e11874, 2022. https://doi.org/10.1016/j.heliyon.2022.e11874.

[9] S. Das, S. Raj, and V. Kumar. On topological indices of molnupiravir and its qspr modelling with some other antiviral drugs to treat covid-19 patients. *Journal of Mathematical Chemistry*, 62:2581–2624, 2024. https://doi.org/10.1007/s10910-023-01518-z.

[10] A. DS. Physiochemical properties of benzophenone and curcumin-conjugated pamam dendrimers using topological indices. *Polycyclic Aromatic Compounds*, 44(5):3419–3441, 2024. https://doi.org/10.1080/10406638.2023.2234542.

[11] S. M. Free and J. W. Wilson. A mathematical contribution to structure-activity studies. *Journal of Medicinal Chemistry*, 7(4):395–399, 1964. https://doi.org/10.1021/jm00334a001.

[12] L. Gnanaraj, D. Ganesan, and M. Siddiqui. Topological indices and qspr analysis of nsaid drugs. *Polycyclic Aromatic Compounds*, 43:9479–9495, 2023. https://doi.org/10.1080/10406638.2022.2164315.

[13] E. Gopal and V. Maheswari. Some labeling for duplicate graph of double quadrilateral flow graph. *Journal of Physics: Conference Series*, 1362:012054, 2019. https://doi.org/10.1088/1742-6596/1362/1/012054.

[14] M. Guo, L. Xu, C.-Y. Hu, and S.-M. Yu. Study on structure-activity relationship of orgonic compounds-applications of a new highly discriminating topological index. *Communications in Mathematical and in Computer Chemistry*, 35:185–197, 1997.

[15] A. Hakeem, F. Nek Muhammad Kabar Muhammad, and N. Ahmed. On the molecular structure modelling of gamma graphyne and armchair graphyne nanoribbon via reverse degree-based topological indices. *Molecular Physics*, 122(5):e2259510, 2023. https://doi.org/10.1080/00268976.2023.2259510.

[16] A. Hakem. Qspr analysis of some novel drugs used for cardiovascular diseases through degree-based topological indices and regression models. *Research Square*, 2023. https://doi.org/10.21203/rs.3.rs-3576948/v1.

[17] W. Harry. Structural determination of paraffin boiling points. *Journal of the American Chemical Society*, 69(1):17–20, 1947.

[18] O. Havare. Qspr analysis with curvilinear regression modeling and topological indices. *Iranian Journal of Mathematical Chemistry*, 10(4):331–341, 2019. https://doi.org/10.22052/ijmc.2019.191865.1448.

[19] S. Hayat, S. Alanazi, and J.-B. Liu. Two novel temperature-based topological indices with strong potential to predict physicochemical properties of polycyclic aromatic hydrocarbons with applications to silicon carbide nanotubes. *Physica Scripta*, 99:55027, 2024. https://doi.org/10.1088/1402-4896/ad3ada.

[20] S. Hayat, H. Mahadi, S. Alanazi, and S. Wang. Predictive potential of eigenvalues-based graphical indices for determining thermodynamic properties of polycyclic aromatic hydrocarbons with applications to polyacenes. *Composites Science and Technology*, 238:112944, 2024. https://doi.org/10.1016/j.compscitech.2024.112944.

[21] L. Huang, Y. Wang, K. Pattabiraman, P. Danesh, M. Siddiqui, and M. Cancan. Topological indices and qspr modeling of new antiviral drugs for cancer treatment. *Polycyclic Aromatic Compounds*, 43:8147–8170, 2023. https://doi.org/10.1080/10406638.2022.2145320.

[22] R. Huang, M. Kamran, S. Manzoor, and S. Ahmad. On eccentricity-based entropy measures for dendrimers. *Heliyon*, 7(8):e07762, 2021. https://doi.org/10.1016/j.heliyon.2021.e07762.

[23] W. Hui, M. Siddiqui, S. Akhter, S. Hafeez, and Y. Ali. On degree-based topological aspects of some dendrimers. *Polycyclic Aromatic Compounds*, 43:3601–3612, 2023. https://doi.org/10.1080/10406638.2022.2074478.

[24] P. Indira and K. Thirusangu. L (3, 1) - labeling for some extended duplicate graphs. *Journal of Emerging Technologies and Innovative Research*, 7(11):383–393, 2002.

[25] O. Ivacciuc. Chemical graphs, molecular matrices and topological indices in chemoinformatics and quantitative structure-activity relationships. *EurekaSelect*, 9(2):153–163, 2013. http://www.eurekaselect.com/article/52866.

[26] O. IVANCIUC. Design of topological indices. part 14. *Revue Roumaine de Chimie*, 45(6):587–596, 2000.

[27] A. Jabeen, S. Ahmad, and S. Zaman. The study of regression model based on com-polynomial in blood cancer drug properties. *Partial Differential Equations in Applied Mathematics*, 9:100648, 2024. https://doi.org/10.1016/j.padiff.2024.100648.

[28] D. Janežič, A. Miličević, S. Nikolić, and N. Trinajstić. *Graph Theoretical Matrices in Chemistry*, volume 3. Jan. 2007. https://doi.org/10.1201/b18389.

[29] N. Kansal, P. Garg, and O. Singh. Temperature-based topological indices and qspr analysis of covid-19 drugs. *Polycyclic Aromatic Compounds*, 43:4148–4169, 2023. https://doi.org/10.1080/10406638.2022.2086271.

[30] J. Labanowski, I. Motoc, and R. Dammkoehler. The physical meaning of topological indices. *Computers & Chemistry*, 15(1):47–53, 1991. https://doi.org/10.1016/0097-8485(91)80023-F.

[31] J.-B. Liu, D. Xavier, E. Varghese, A. Baby, and D. Mathew. Molecular descriptors of porphyrin-based dendrimer. *Polycyclic Aromatic Compounds*, 43:6126–6137, 2023. https://doi.org/10.1080/10406638.2022.2112714.

[32] J.-B. Liu, D. A. Xavier, E. S. Varghese, A. Baby, and D. Mathew. Molecular descriptors of porphyrin-based dendrimer. *Polycyclic Aromatic Compounds*, 43(7):6126–6137, 2023.

[33] P. Liu and W. Long. Current mathematical methods used in qsar/qspr studies. *International Journal of Molecular Sciences*, 10(2):1978–1998, 2009. https://doi.org/10.3390/ijms10051978.

[34] M. Malik, M. Binyamin, and S. Hayat. Correlation ability of degree-based topological indices for physicochemical properties of polycyclic aromatic hydrocarbons with applications. *Polycyclic Aromatic Compounds*, 42:6267–6281, 2022. https://doi.org/10.1080/10406638.2021.1977349.

[35] O. Mekenyan and S. Basak. Topological indices and chemical reactivity. In *Graph Theoretical Approaches to Chemical Reactivity*, pages 221–239. 1994. https://doi.org/10.1007/978-94-011-1202-4_8.

[36] O. Mekenyan and S. Basak. Topological indices and chemical reactivity. In *Graph Theoretical Approaches to Chemical Reactivity*, volume 9, 1994. https://doi.org/10.1007/978-94-011-1202-4_8.

[37] S. Mondal, A. Dey, N. De, and A. Pal. Qspr analysis of some novel neighbourhood degree-based topological descriptors. *Complex and Intelligent Systems*, 7:977–996, 2021. https://doi.org/10.1007/s40747-020-00262-0.

[38] U. Muhammad and J. Muhammad. Connection-based zagreb indices of polycyclic aromatic hydrocarbons structures. *Current Organic Synthesis*, 21(3):246–256, 2024. http://dx.doi.org/10.2174/1570179421666230823141758.

[39] G. Murugan, K. Julietraja, and A. Alsinai. Computation of neighborhood m-polynomial of cycloparaphenylene and its variants. *ACS Omega*:1–9, 2023. https://doi.org/10.1021/acsomega.3c07294.

[40] S. Nagarajan, G. Priyadharshini, and K. Pattabiraman. Qspr modeling of status-based topological indices with covid-19 drugs. *Polycyclic Aromatic Compounds*, 43:6868–6887, 2023. https://doi.org/10.1080/10406638.2022.2127803.

[41] S. P, N. Singh, D. Mishra, S. Ehsan, V. Chaturvedi, A. Chaudhary, V. Singh, and E. Vamanu. Computational approaches to designing antiviral drugs against covid-19: a comprehensive review. *Current Pharmaceutical Design*, 29:2601–2617, 2023. https://doi.org/10.2174/0113816128259795231023193419.

[42] K. Pattabiraman and M. Cancan. Qspr modeling with topological indices of some potential drugs against cancer. *Polycyclic Aromatic Compounds*, 44(2):1181–1208, 2023. https://doi.org/10.1080/10406638.2023.2189270.

[43] M. Rahul, J. Clement, J. Singh Junias, M. Arockiaraj, and K. Balasubramanian. Degree-based entropies of graphene, graphyne and graphdiyne using shannon's approach. *Journal of Molecular Structure*, 1260:132797, 2022. https://doi.org/10.1016/j.molstruc.2022.132797.

[44] V. Ravi and K. Desikan. Curvilinear regression analysis of benzenoid hydrocarbons and computation of some reduced reverse degree based topological indices for hyaluronic acid-paclitaxel conjugates. *Scientific Reports*, 13:1–14, 2023. https://doi.org/10.1038/s41598-023-28416-3.

[45] J. Rodríguez-Velázquez and A. Balaban. Two new topological indices based on graph adjacency matrix eigenvalues and eigenvectors. *Journal of Mathematical Chemistry*, 57(6):1053–1074, 2019. https://doi.org/10.1007/s10910-019-01008-1.

[46] E. Sampathkumar. On duplicate graphs. *The Journal of the Indian Mathematical Society*, 37:285–293, 1974.

[47] M. Sardar, M. Ali, M. Farahani, M. Alaeiyan, M. Cancan, and Z. Campus. Topological indices and qspr / qsar analysis of some drugs being investigated for the treatment of headaches. *European Chemical Bulletin*, 12:69–83, 2023.

[48] J. Senbagamalar, A. Meenakshi, A. Kanchana, and H. Hachimi. Topological indices on central graph. In *Proceedings of 2nd International Conference on Mathematical Modeling and Computational Science*, volume 1422, pages 427–433, 2022. https://doi.org/10.1007/978-981-19-0182-9_43.

[49] A. Shabbir. Computing and comparative analysis of topological invariants of symmetrical carbon nanotube y junctions. *Arabian Journal of Chemistry*, 15(1):103509, 2022. https://doi.org/10.1016/j.arabjc.2021.103509.

[50] M. Shanmukha, N. Basavarajappa, K. Shilpa, and A. Usha. Degree-based topological indices on anticancer drugs with qspr analysis. *Heliyon*, 6(6):e04235, 2020. https://doi.org/10.1016/j.heliyon.2020.e04235.

[51] N. Soleimani, E. Mohseni, N. Maleki, and N. Imani. Some topological indices of the family of nanostructures of polycyclic aromatic hydrocarbons (pahs). *Iranian Journal of Science Foundation*, 46:81–88, 2018. https://doi.org/10.4038/jnsfsr.v46i1.8267.

[52] G. Thamalingam, K. Ponnusamy, A. Ammar, and M. Govindhan. On certain degree based and bond-additive topological indices of dodeca-benzo-circumcoronene. *Combinatorial Chemistry & High Throughput Screening*, 27(11):1629–1641, 2022. http://dx.doi.org/10.2174/0113862073274943231211110011.

[53] K. Thirusangu, P. Ulaganathan, and P. Vijayakumar. Some cordial labeling of duplicate graph of ladder graph. *Annals of Pure and Applied Mathematics*, 8(2):43–50, 2014.

[54] R. Todeschini and V. Consonni. *Handbook of Molecular Descriptors*. John Wiley & Sons, 2008.

[55] D. Truhlar. The concept of resonance. *Journal of Chemical Education*, 84(5):781–782, 2007. https://doi.org/10.1021/ed084p781.

[56] A. Ullah, S. Zaman, A. Hamraz, and M. Muzaammal. On the construction of some bioconjugate networks and their structural modeling via irregularity topological indices. *The European Physical Journal E*, 46:72, 2023. https://doi.org/10.1140/epje/s10189-023-00333-3.

[57] J. Yang, J. Kousalya, and S. Raja. Neighbourhood sum degree-based indices and entropy measures for certain family of graphene molecules. *Molecules*, 28(1):168, 2023. https://doi.org/10.3390/molecules28010168.

[58] S. Zaman, M. Jalani, A. Ullah, M. Ali, and T. Shahzadi. On the topological descriptors and structural analysis of cerium oxide nanostructures. *Chemical Papers*, 77:2917–2922, 2023. https://doi.org/10.1007/s11696-023-02675-w.

[59] S. Zaman, M. Majeed, W. Ahmed, and M. Saleem. On neighbourhood eccentricity-based topological indices and qspr analysis of pahs. *Measurement: Interdisciplinary Research and Perspectives*:1–14, 2024. https://doi.org/10.1080/15366367.2024.2329950.

[60] S. Zaman, A. Ullah, and A. Shafaqat. Structural modeling and topological characterization of three kinds of dendrimer networks. *The European Physical Journal E*, 46:36, 2023. https://doi.org/10.1140/epje/s10189-023-00297-4.

[61] X. Zhang, M. Saif, N. Idrees, S. Kanwal, S. Parveen, and F. Saeed. Qspr analysis of drugs for treatment of schizophrenia using topological indices. *ACS Omega*, 8:41417–41426, 2023. https://doi.org/10.1021/acsomega.3c05000.